Renormalization of crossing probabilities in the dilute Potts model

Pete Rigas

November 14, 2020

1 Introduction

Russo-Seymour-Welsh (RSW) theory provides estimates regarding the crossing probabilities across rectangles of specified aspect ratios, and was studied by Russo, and then by Seymour and Welsch on the square lattice, with results specifying the finite mean size of percolation clusters [23], in addition to a relationship that critical probabilities satisfy through a formalization of the sponge problem [24]. With such results, other models in statistical physics have been examined, particularly ones exhibiting sharp threshold phenomena [1,7] and continuous phase transitions [13], with RSW type estimates obtained for Voronoi percolation [27], critical site percolation on the square lattice [28], the Kostlan ensemble [2], and the FK Ising model [9], to name a few.

RSW arguments typically rely on self-duality of the model, in which the probability of obtaining a horizontal crossing is related, by duality, to the probability of obtaining a vertical crossing. Although this correspondence is useful for models enjoying self duality, previous arguments to obtain RSW estimates are not applicable to the dilute Potts model (in correspondence with the loop $O(n)$ model in presence of two external fields), which has been studied extensively by Nienhuis [15,19,20] who not only conjectured that the critical point of the model should be $1/\sqrt{2+\sqrt{2-n}}$ for $0 \leq n < 2$, but also has provided results for the $O(n)$ model on the honeycomb lattice [22] which has connective constant $\sqrt{2+\sqrt{2}}$ [12]. It is also known that the loop $O(n)$ model, a model for random collections of loop configurations on the hexagonal lattice, exhibits a phase transition with critical parameter $1/\sqrt{2+\sqrt{2-n}}$, in which *subcritically* the probability of obtaining a macroscopic loop configuration of length k decays exponentially fast in k, while *at criticality* the probability of obtaining infinitely many macroscopic loop configurations, also of length k, and centered about the origin is bound below by c and above by $1-c$ for $c \in (0,1)$ irrespective of boundary conditions [8]. The existence of macroscopic loops in the loop $O(n)$ model has also been proved in [3] with the XOR trick.

In another recent work [14], Duminil-Copin *&* Tassion proposed alternative arguments to obtain RSW estimates for models that are no self-dual. The novel quantities of interest in the argument involve renormalization inequalities, which in the case of Bernoulli percolation can be viewed as a coarse graining argument, as well as the introduction of strip densities which are quantities defined as a limit supremum over a real parameter α. Ultimately, the paper proves RSW estimates for measures with free or wired boundary conditions in *subcritical, supercritical, critical discontinuous & critical continuous* cases, with applications of the two theorems relating to the mixing times of the random cluster measure, for systems undergoing discontinuous phase transitions [14,18]. Near the end of the introduction, the authors mention that potential generaliations of their novel renormalization argument can be realized in the dilute Potts model studied by Nienhuis which is equivalent to the loop $O(n)$ model, a model conjectured to exist in the same universality class as the spin $O(n)$ model.

With regards to the loop $O(n)$ model, previous arguments have demonstrated that the model undergoes a phase transition by making use of Smirnov's *parafermionic observable*, which was originally introduced to study conformal invariance of different models in several celebrated works [11,25,26]. As a holomorphic function, the discrete contour integral of the observable vanishes for specific choice of a multiplicative parameter to the winding term in the power of the exponential. Under such assumptions on σ, Duminil-Copin & friends prove exponential decay in the loop $O(n)$ model from arguments relating to the relative weights of paths and a discretized form of the Cauchy Riemann equations which is shown to vanish [8]. Historically, disorder operators share connections with the parafermionic observable and have been studied to prove the existence of phase transitions through examination of the behavior of expectations of random variables below, and above, a critical point [11,16], while other novel uses of the parafermionic observable have been introduced in [10].

2 Background

To execute steps of the renormalization argument in the hexagonal case, we introduce quantities to avoid making use of self duality arguments. For $G=(V,E)$, $n \geq 1$ and the strip $\mathbf{R} \times [-n, 2n] \equiv S_n \subset G$, let $\phi^{\xi}_{S_n}$, for $\xi \in \{0,1,0/1\}$, respectively denote the measures with free, wired and Dobrushin boundary conditions in which all vertices at the bottom of the strip are wired. From such measures on the square lattice, several planar crossing events are defined in order to obtain RSW estimates for all four parameter regimes (*subcritical, supercritical, discontinuous & continuous critical*), including analyses of the intersection of crossing probabilities across a family of non disjoint rectangles $\mathcal{R}$, each of aspect ratio $[0,\rho n] \times [0,n]$ for $\rho > 0$, to obtain crossings across long rectangles á la FKG inequality, three arm events which establish lower bounds of the crossing probabilities across $\mathcal{R}$ under translation and reflection invariance of ϕ, in addition to horizontal rectangular crossings which are used to prove renormalization inequalities through use of PushPrimal & PushDual relations. To begin, we define the horizontal and vertical crossing strip densities.

Definition ([14, Theorem 2 & Corollary 3]): The *strip density* corresponding to the measure across a rectangle $\mathcal{R}$ of aspect ratio $[0,\alpha n] \times [-n,2n]$ with free boundary conditions is of the form,

$$p_n = \limsup_{\alpha \to \infty} \left(\phi^0_{[0,\alpha n]\times[-n,2n]}[\mathcal{H}_{[0,\alpha n]\times[0,n]}] \right)^{\frac{1}{\alpha}} ,$$

where $\mathcal{H}$ denotes the event that $\mathcal{R}$ is crossed horizontally, whereas for the measure supported over $\mathcal{R}$ with wired boundary conditions, the crossing density is of the form,

$$q_n = \limsup_{\alpha \to \infty} \left(\phi^1_{[0,\alpha n]\times[-n,2n]}[\mathcal{V}^c_{[0,\alpha n]\times[0,n]}] \right)^{\frac{1}{\alpha}} ,$$

where $\mathcal{V}^c$ denotes the complement of a vertical crossing across $\mathcal{R}$.

Besides the definition of the strip densities p_n and q_n, another key step in the argument involves inequalities relating p_n and q_n. The statement of the Lemma below holds under the assumption that the planar random cluster model is neither in the subcritical nor supercritical phase.

Lemma 1 ([14, Lemma 12]) There exists a constant $C>0$ such that for every integer $\lambda \geq 2$, and for every $n \in 3\mathbf{N}$,

$$p_{3n} \geq \frac{1}{\lambda^C} q_n^{3+\frac{3}{\lambda}} ,$$

while a similar inequality holds between horizontal and the complement of vertical crossing probabilities of the complement $\mathcal{V}^c$ across $\mathcal{R}$, which takes the form,

$$q_{3n} \geq \frac{1}{\lambda^C} p_n^{3+\frac{3}{\lambda}} .$$

Finally, we introduce the renormalization inequalities.

Lemma 2 ([14, Lemma 15]) There exists $C>0$ such that for every integer $\lambda \geq 2$ and for every $n \in 3\mathbf{N}$,

$$p_{3n} \leq \lambda^C p_n^{3-\frac{9}{\lambda}} \;\; \& \;\; q_{3n} \leq \lambda^C q_n^{3-\frac{9}{\lambda}} .$$

To readily generalize the renormalization argument to the dilute Potts model, we proceed in the spirit of [14] by introducing hexagonal analogues of the crossing events discussed at the beginning of the section.

3 Towards hexagonal analogues of crossing events from the planar renormalization argument

3.1 Loop $O(n)$ measure, planar crossing event types

The Gibbs measure on a random configuration σ in the loop $O(n)$ model is of the form,

$$\mathbf{P}^{\xi}_{\Lambda,x,n}(\sigma) = \frac{x^{e(\sigma)} n^{l(\sigma)}}{Z^{\xi}_{\Lambda,x,n}} , \qquad \text{(Loop measure)}$$

where $\sigma(e)$ denotes the number of edges, $\sigma(l)$ the number of loops, $\Lambda \subset \mathbf{H}$, $\xi \in \{0, 1, 0/1\}$ and $Z^{\xi}_{\Lambda,e,n}$ is the partition function which normalizes $\mathbf{P}^{\xi}_{\Lambda,x,n}$ so that it is a probability measure. In particular, we restrict the parameter regime of x to that of [8], in which the loop $O(n)$ model satisfies the strong FKG lattice condition and monotonicity through a spin representation measure albeit $\mathbf{P}^{\xi}_{\Lambda,x,n}$ not being monotonic. By construction, $\mathbf{P}^{\xi}_{\Lambda,x,n}$ is invariant under $\frac{2\pi}{3}$ rotations. Through a particular extension for $n \geq 2$ of the spin representation of $\mathbf{P}^{\xi}_{\Lambda,\sigma(e),\sigma(l)}$, the measure on spin configurations $\sigma' \in \Sigma(G, \tau)$ is of the form

$$\mu^{\tau}_{G,x,n}(\sigma') = \frac{n^{k(\sigma')} x^{e(\sigma')} e^{hr(\sigma') + \frac{h'}{2} r'(\sigma')}}{Z^{\tau}_{G,x,n}} , \qquad \text{(Spin measure)}$$

where $\tau \in \{-1, +1\}^{\mathbf{T}}$, $\Sigma(G, \tau)$ is the set of spin configurations coinciding with σ' outside of G, $r(\sigma') = \sum_{u \in G} \sigma'_u$ is the summation of spins inside G, $r'(\sigma') = \sum_{\{u,v,w\} \in G} \sigma'_u \mathbf{1}_{\sigma'_u = \sigma'_v = \sigma'_w}$ is the difference between the spins of monochromatic triangles, and $Z^{\tau}_{G,n,x}$ is the partition function which makes $\mu^{\tau}_{G,x,n}$ a probability measure. The extension enjoys translation invariance, a weaker form of the spatial/domain Markov property that will be mentioned in *Section* 5.1, comparison between boundary conditions that is mentioned in *Section* 3.2, & FKG for $n \geq 1$ and $nx^2 \leq 1$. The dual measure of $\mu^{+1}_{G,x,n}$ is $\mu^{0}_{G^*,x,n}$. Simply put, the superscripts above μ indicate whether the pushforward of a horizontal or vertical crossing event under the measure is under free, wired, or mixed boundary conditions.

To obtain boundary dependent RSW results on $\mathbf{H}$ in all 4 cases, we identify crossing events in the planar renormalization argument in addition to difficulties associated with applying the planar argument to the push forward of similarly defined horizontal and vertical crossing events under $\mu^{\tau}_{G,x,n}$ on $(\mathbf{T})^* = \mathbf{H}$. In what follows, we describe all planar crossing events in the argument.

First, planar crossing events across translates of horizontal crossings across short rectangles of equal aspect ratio are combined to obtain horizontal crossings across long rectangles, through the introduction of a lower bound to the probability of the intersection that all short rectangles are simultaneously crossed horizontally with FKG. On $\mathbf{H}$, the probability of the intersection of horizontal crossing events of **first type** can be readily generalized to produce longer horizontal crossings from the intersection of shorter ones, through an adaptation of [14, Lemma 9].

Second, three arm events which determine whether two horizontal crossings to the top of a rectangle of aspect ratio $[0, n] \times [0, \rho n]$ intersect. Planar crossings of **second type** create symmetric domains over which the conditional probability of horizontal crossings in the symmetric domain can be determined, which for the renormalization argument rely on comparison between random cluster measures with free and wired boundary conditions. For random cluster configurations, comparison between boundary conditions is established in how the number of clusters in a configuration is counted. Comparison between boundary conditions applies to $\mu^{\tau}_{G,x,n}$ from [8], with hexagonal symmetric domains enjoying $\frac{2\pi}{3}$ symmetry.

Third, planar crossing events with wired boundary conditions, of **third type** induce wired boundary conditions within close proximity of vertical crossings in planar strips. Long planar horizontal crossings are guaranteed through applications of FKG across dyadic translates of horizontal crossings across shorter rectangles. For hexagonal domains, modifications to planar crossings of **first type** permit ready generalizations of **third type** planar crossings.

Fourth, planar horizontal crossing events of **fourth type** across rectangles establish relations between the strip densities p_n & q_n (**Lemma 1**). Finally, planar crossing events satisfying PushPrimal & PushDual conditions prove **Lemma 2**.

3.2 Comparison of boundary conditions & relaxed spatial markovianity for the $n \geq 2$ extension of the loop $O(n)$ measure

For suitable comparison of boundary conditions in the presence of external fields h, h', the influence of boundary conditions from the fields on the spin representation amount to enumerating configurations differently for wired and free boundary conditions than for the random cluster model in [14]. In particular, modifications to comparison between boundary conditions and the spatial Markov property.

Chiefly, the modifications entail that an admissible symmetric domain Sym inherit boundary conditions from partitions on the outermost layer of hexagons along loop configurations (see *Figures 1-3* in later section for a visualization of crossing events from the argument). Through distinct partitions of the $+/-$ assignment on hexagons on the outermost layer to the boundary, appearing in arguments for symmetric domains.

.

Altogether, modifications to comparison of boundary conditions and the spatial Markov property between measureable spin configurations for μ are achieved. Denote the modified properties for spin representations $\mathcal{S}$ with ($\mathcal{S}$ CBC) and ($\mathcal{S}$ SMP).

3.3 Results

The result presented for the loop $O(n)$ model mirrors the dichotomy of possible behaviors, in which the *standard box crossing estimate* reflects the influence of boundary conditions on the nature of the phase transition, namely that the transition is discontinuous, from the *discontinuous critical* case. To prove the *subcritical* & *supercritical* cases, the generalization to the dilute Potts model will make use of planar crossing events of **first** and **second** type, while crossing events of **third** and **fourth** type proves the remaining *continuous & discontinuous critical* cases. We denote the vertical strip domain $\mathcal{S}_T$ with T hexagons, $\mathcal{S}_{T,L}$ the finite domain of $\mathcal{S}_T$ of length $\pm L > 0$, and any regular hexagon $H_j \subset \mathcal{S}_T$ with side j [12].

Theorem 1^* (*μ homeomorphism*): For $L \in [0,1]$, there exits an increasing homeomorphism f_L so that for every $n \geq 1$, where $\mathcal{H}_H \equiv \mathcal{H}$ and $\mathcal{V}_H \equiv \mathcal{V}$ denote the horizontal and vertical crossings across a regular hexagon H, $\mu(\mathcal{H}) \geq f(\mu(\mathcal{V}))$.

Theorem 2^* (*hexagonal crossing probabilities*): For the dilute regime $x \leq \frac{1}{\sqrt{n}}$, aspect ratio n of a regular hexagon $H \subset \mathcal{S}_T$, $c > 0$, and horizontal crossing $\mathcal{H}$ across H, estimates on crossing probabilities with free, wired or mixed boundary conditions satisfy the following criterion in the following **4** possible behaviors.

- *Subcritical*: For every $n \geq 1$, under wired boundary conditions, $\mu^1_{G,x,n}[\mathcal{H}] \leq \exp(-cn)$,
- *Supercritical*: For every $n \geq 1$, under free boundary conditions, $\mu^0_{G,x,n}[\mathcal{H}] \geq 1 - \exp(-cn)$,
- *Continuous Critical* (*Russo-Seymour-Welsh property*): For every $n \geq 1$, independent of boundary conditions τ, $c \leq \mu^\tau_{G,x,n}[\mathcal{H}] \leq 1 - c$,
- *Discontinuous Critical*: For every $n \geq 1$, $\mu^1_{G,x,n}[\mathcal{H}] \geq 1 - \exp(-cn)$ for free boundary conditions, while $\mu^0_{G,x,n}[\mathcal{H}] \leq \exp(-cn)$ for wired boundary conditions.

Lemma 1^* (*hexagonal strip density inequalities*):

Lemma 2^* (*hexagonal renormalization inequalities*):

4 Proof of Theorem 1 & Lemma 9^* preparation

To prove Theorem 1, we introduce 6-arm crossing events, from which symmetric domains will be crossed with good probability. The arguments hold for the $n \geq 2$ extension measure with free, wired or mixed boundary conditions. Previous use of such domains has been implemented to avoid using self duality throughout the renormalization argument [1,13]. Although more algebraica characterizations of fundamental domains on the hexagonal, and other, lattices exist [4], we focus on defining crossing events, from which we compute the probability conditioned on a path Γ crossing the symmetric region.

4.1 Existence of f

The increasing homeomorphism is shown to exist with the following.

Proposition 8^* (*homeomorphism existence*): For any $L > 0$, there exists $c_0 = c_0(L) > 0$ so that for $nL \geq 1$, $\mu[\mathcal{H}] \geq c_0 \mu[\mathcal{V}]^{\frac{1}{c_0}}$.

Proof of Theorem 1^*. With the statement of 8^*, for $\mu = \mu^\tau$ on $\mathcal{S}_{T,L}$, μ^* is a measure supported on dual loop configurations, from which a correspondence between horizontal and vertical hexagonal crossings is well known. Trivially, by making use of 8^*, rearrangements across the following inequality demonstrate the existence of f that is stated in *Theorem 1*, as

$$\mu^*[\mathcal{H}] \geq c_0 \mu^*[\mathcal{V}]^{\frac{1}{c_0}} \Leftrightarrow 1 - \mu[\mathcal{V}] \geq c_0 \bigg(1 - \mu[\mathcal{H}]\bigg)^{\frac{1}{c_0}} \Leftrightarrow \bigg(1 - \mu[\mathcal{V}]\bigg)^{c_0} \geq c_0^{c_0} \bigg(1 - \mu[\mathcal{H}]\bigg) \Leftrightarrow \mu[\mathcal{H}] \leq 1 - \frac{1}{c_0^{c_0}} \bigg(1 - \mu[\mathcal{V}]\bigg) ,$$

because by duality, $\mu[\mathcal{H}] + \mu^*[\mathcal{V}] = 1$. The homeomorphism can be read off from the inequality, hence establishing its existence. $\square$

4.2 Crossing events for Lemma 9^*

For a fixed ordering of all 6 edges that enclose any $H_j \subset \mathcal{S}_{T,L}$, $\{1_j, 2_j, 3_j, 4_j, 5_j, 6_j\}$, crossing events $\mathcal{C}$ to obtain hexagonal symmetric domains with rotational and reflection symmetry will be defined. To obtain generalized regions from their symmetric counterparts in the plane from [14], we make use of comparison between boundary condition with the $n \geq 2$ extension measure. For μ, we are capable of readily proving a generalization of the union bound with the following prescription.

First, we define 6 armed crossing events across arbitrary $H_j \in \mathcal{S}_{T,L}$, from which countable families of crossing probabilities are introduced. The construction of the families is dependent on a partition of a single edge of H_j which we denote without loss of generality as edge 1_j of H_j. After partitioning 1 into equal k subintervals, each of length $\frac{s}{k}$, we define a countable family of crossing events from the partition $\mathcal{S}_j$ of 1_j to the corresponding topmost edge 4_j of H_j, as well as crossing events from $\mathcal{S}_j$ to all remaining edges of H_j. We also introduce a standard formulation of the union bound for the family of crossing events which has a lower bound dependent on the probability of a vertical hexagonal crossing. For our choice of 1_j, we position a horizontal line $\mathcal{L} \equiv [0, \delta] \times \{0\} \subset \mathbf{H}$ for arbitrary δ, from which we denote the horizontal translate $H_{j+\delta'}$ of H_j horizontally along $\mathcal{L}$ by δ' where the magnitude of the translation satisfies $\delta' << \delta$. Second, across the countable family of crossing pairs for any sequence of 3 hexagons $\{H_{j-\delta'}, H_j, H_{j+\delta'}\}$, we define additional crossing events across the hexagonal translates through the stipulation that the crossing starting from an arbitrary partition of 1 to any of the remaining edges $\{2, 3, 4, 5, 6\}$ of H occur in the intermediate regions $H_{j-\delta'} \cap H_j$ and $H_j \cap H_{j+\delta'}$ [1] (respectively given by the nonemtpy intersection between the gray and blue hexagons, and blue and red hexagons, in *Figure 1* on the top of the next page) for $j > 0$. Third, we accommodate higher degrees of freedom in the number of arms for hexagonal events by reducing the number of crossing events taken in the maximum for the union bound, in turn reducing the 9^* proof to three distinct cases. We generalize the argument to the dilute Potts model, which can be placed into correspondence with the loop $O(n)$ model, by accounting for the $+/-$ spin representation from the extension μ. Fourth, we introduce adaptations to the renormalization argument across the remaining hexagonal domains. Finally, we let $L \to \infty$, and generalize the crossing events on $\mathcal{S}_T$ in the weak limit along the infinite hexagonal strip.

Differences emerge in the proofs for the dilute Potts model in comparison to those of the random cluster model, not only in the encoding of boundary conditions for μ but also in the construction of the family of crossing probabilities, and the cases that must be considered to prove the union bound. We gather these notions below; denote the quantities corresponding to the partition $\mathcal{S}_j \subset 1_j$ with the following events,

$$\mathscr{C}_{2_j} = \{\mathcal{S}_j \overset{H_{j+\delta'}}{\longleftrightarrow} 2_{j-\delta'}\}, \mathscr{C}_{3_j} = \{\mathcal{S}_j \overset{H_{j+\delta'}}{\longleftrightarrow} 3_{j-\delta'}\} \ , \ \mathscr{C}_{4_j} = \{\mathcal{S}_j \overset{H_j}{\longleftrightarrow} 4_j\}, \mathscr{C}_{5_j} = \{\mathcal{S}_j \overset{H_{j-\delta'}}{\longleftrightarrow} 5_{j+\delta'}\} \ , \ \& \ \ \mathscr{C}_{6_j} = \{\mathcal{S}_j \overset{H_{j-\delta'}}{\longleftrightarrow} 6_{j+\delta'}\},$$

as well as the following crossing events across the left and right translates of H_j,

[1] In comparison to the argument of [14] which demands that crossings occur in between segments $S_2 \cup S_4$ in a rectangle R_0, we introduce an auxiliary parameter δ' when defining crossing events.

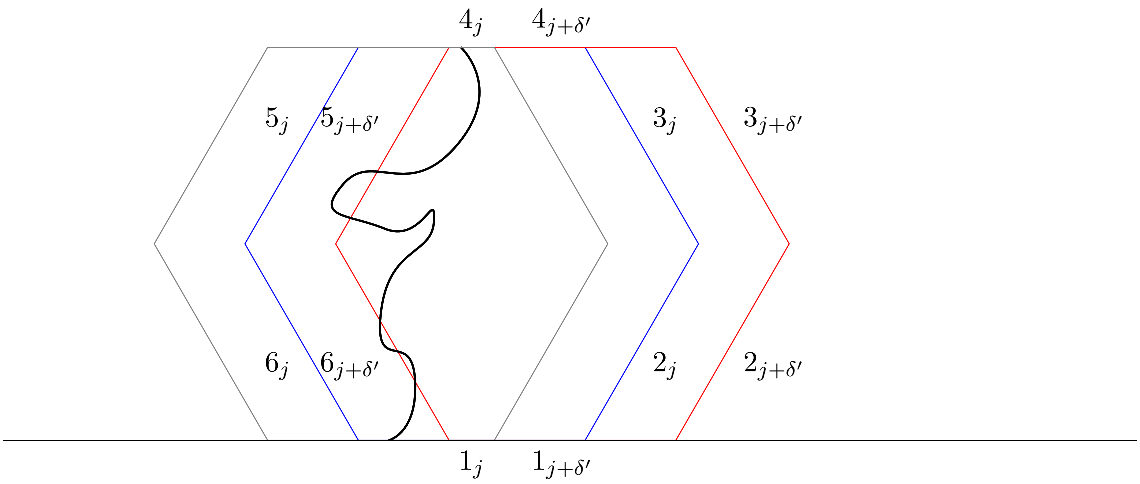

Figure 1: *The centermost blue hexagon H_j flanked by its gray left translate $H_{j-\delta'}$, and its red right translate $H_{j+\delta'}$. 1_j lies incident to $\mathcal{L}$ for every point on the edge. A vertical crossing from the partition $\mathcal{S}_j \subset 1_j$ to 4_j is shown.*

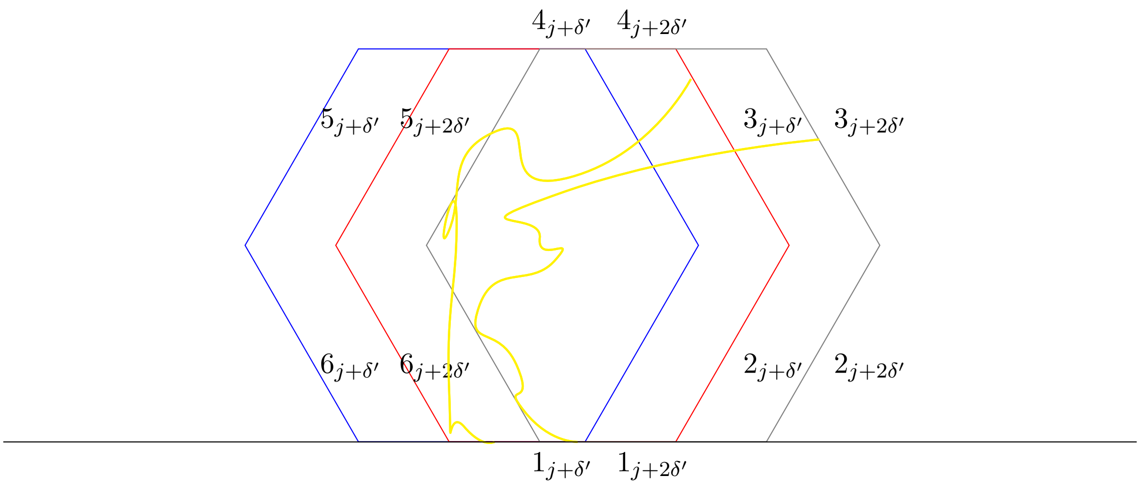

Figure 2: *Yellow crossings from the partition $\mathcal{S}_{j+\delta'} \subset 1_{j+\delta'}$ to $3_{j+\delta'}$, and from the partition $\mathcal{S}_{j+2\delta'} \subset 1_{j+2\delta'}$ to $3_{j+2\delta'}$ are shown. We neglect illustrating additional connected components of loop configurations above in $H_{j-\delta'}, H_j$ or $H_{j+\delta'}$ beyond the intersection of the paths with $3_{j+\delta'}$, as the paths would necessarily have to traverse leftwards so that the crossings respectively occur in H_j and $H_{j+\delta'}$. Under $\frac{2\pi}{3}$ rotational invariance of μ, symmetric domains contructed for $\mathscr{C}_{3_j}$ correspond to those for $\mathscr{C}_{6_j}$.*

$$\mathscr{C}'_{2_j} = \{\mathcal{S}_j \overset{H_{j+\delta'}}{\longleftrightarrow} 2_{j+\delta'}\} \setminus \mathscr{C}_{2j} \; , \mathscr{C}'_{3_j} = \{\mathcal{S}_j \overset{H_{j+\delta'}}{\longleftrightarrow} 3_{j+\delta'}\} \setminus \mathscr{C}_{3j} \; ,$$
$$\mathscr{C}'_{5_j} = \{\mathcal{S}_j \overset{H_{j-\delta'}}{\longleftrightarrow} 5_{j+\delta'}\} \setminus \mathscr{C}_{5j} \; , \mathscr{C}'_{6_j} = \{\mathcal{S}_j \overset{H_{j-\delta'}}{\longleftrightarrow} 6_{j+\delta'}\} \setminus \mathscr{C}_{6j} \; .$$

Along with the right and left translates of H_j, we can easily Before proceeding to make use of the 6-arm events to create symmetric domains for Lemma 9* (presented below), we briefly prove 8*.

Proof of Proposition 8*. Let $C_j = \{\mathcal{S}_j \overset{H_j \cup H_{j+2\delta'}}{\longleftrightarrow} \mathcal{S}_{j+\delta'} \cup \mathcal{S}_{j+2\delta'}\}$. Uniformly in boundary conditions, for 8* horizontal (vertical) crossings $\mathcal{H}$ ($\mathcal{V}$) across H_j can be pushed forwards under μ to obtain a standard lower bound for the probability of obtaining a longer vertical (horizontal) crossing $\mathcal{V}'$ ($\mathcal{H}'$) through one application of FKG to the finite intersection of shorter vertical (horizontal) crossings $\mathcal{H}'_j$ ($\mathcal{V}'_j$),

$$\mu[\mathcal{H}'] \geq \mu\bigg(\bigcap_{j \in \mathcal{J}} C_j\bigg) \geq \prod_{j \in \mathcal{J}} \mu[\mathcal{V}'_j] \geq \bigg(\frac{c}{\lambda^5}\mu[\mathcal{V}']^5\bigg)^{|\mathcal{J}|} \; ,$$

where the product is taken over admissible $j \in \mathcal{J} \equiv \{j \in \mathbf{R} :$ there exists a regular hexagon with side length j & $H_j \cap \mathcal{S}_{T,L} \neq \emptyset\}$, with $c, \lambda > 0$. From a standard lower bound from vertical crossings, the claim follows by setting λ equal to the aspect ratio of H_j. $\square$

We turn to a statement of 9^*.

Lemma 9^* (6-*arm lower bound, existence of* c): For every $\lambda > 0$ there exists a constant c, λ such that for every $n \in \mathbf{Z}$,

$$\mu[C_0] \geq \frac{c}{\lambda^5} \mu[\mathcal{V}']^5 \ .$$

5 9^* arguments

Proof of Lemma 9^*. For the 6-*arm lower bound*, the argument involves manipulation of symmetric domains. In particular, we must examine the crossing event that is the most probable from the union bound, in 3 cases that are determined by the $\frac{2\pi}{3}$ rotational invariance of μ. Under this symmetry, in the union bound it is necessary that we only examine the structure of the crossing events $\mathcal{C}$ in the following cases. We include the index j associated with crossing events $\mathcal{C}_j$, executing the argument for arbitrary j (in contrast to $j \equiv 0$ in [14]), readily holding for any triplet $j - \delta', j, j + \delta'$. Besides exhibiting the relevant symmetric domain in each case, the existence of c will also be justified. We partition Sym into 4 parts, L_{Sym}, R_{Sym}, T_{Sym} and B_{Sym}.

5.1 $\mathcal{C}_j \equiv \mathscr{C}_{2_j}$

In the first case, crossings across 2_j can be analyzed with the events $\mathscr{C}_j$ and $\mathscr{C}_{j+2\delta'}$. To quantify the conditional probability of obtaining a $2_{j+\delta'}$ crossing beginning from $\mathcal{S}_{j+\delta'}$, let Γ_{2_j} and $\Gamma_{2_{j+2\delta'}}$ be the set of respective paths from $\mathcal{S}_j$ and $\mathcal{S}_{j+2\delta'}$ to 2_j and $2_{j+2\delta'}$, and also realizations of the paths as $\gamma_1 \in \Gamma_{2_j}$, $\gamma_2 \in \Gamma_{2_{j+2\delta'}}$.

To accommodate properties of the dilute Potts model, we also condition that the number of connected components k_{γ_1} of γ_1 equal the number of connected components of k_{γ_2} of γ_2 in the spin configuration sampled under μ (see *Figure 3* for one example, in which the illustration roughly gives one half of the top part of Sym which is above the point of intersection x^{γ_1,γ_2} of the red and purple connected components, while the remaining purple connected components until $x_{\mathcal{I}}$ constitute one half of the lower half of Sym). We denote restrictions of the connected components for γ_1 and γ_2 to the magnified region in *Figure 3*, and with some abuse of notation we still denote $k_{\gamma_1} \equiv k_{\gamma_1}|_{\mathscr{C}_j \cap \mathscr{C}_{j+2\delta'}}$ and $k_{\gamma_2} \equiv k_{\gamma_1}|_{\mathscr{C}_j \cap \mathscr{C}_{j+2\delta'}}$ for simplicity. Finally, assign $\Omega \subset \mathbf{H}$ as the points to the left of γ_1 and to the right of γ_2, and the symmetric domain as $\mathrm{Sym} \equiv \mathrm{Sym}_{2_j} \equiv \mathrm{Sym}_{2_j}(\Omega)$. To obtain a crossing across Sym, we conditionally pushforward the event

$$\mu[C_0 \mid \Gamma_{2_j} = \gamma_1 \ \& \ \Gamma_{2_{j+2\delta'}} = \gamma_2, k_{\gamma_1} = k_{\gamma_2}] \ ,$$

which quantifies the probability of obtaining a connected component across $\mathcal{S}_{j+\delta'} \cup \mathcal{S}_{j+2\delta'}$. We condition C_0 through γ_1 and γ_2 because if there exits a spin configuration passing through Sym whose boundaries are determined by γ_1 and γ_2, then necessarily the configuration would have a connected component from $\mathcal{S}_j$ to $\mathcal{S}_{j+2} \cup \mathcal{S}_{j+4}$ hence confirming that C_0 occurs. To establish a comparison between this conditional probability and the conditional probability of obtaining a horizontal crossing across Sym, consider

$$\mu[\gamma_1 \overset{\Omega}{\longleftrightarrow} \gamma_2 \mid \Gamma_{2_j} = \gamma_1 \ \& \ \Gamma_{2_{j+2\delta'}} = \gamma_2, k_{\gamma_1} = k_{\gamma_2}] \ ,$$

subject to wired boundary conditions on R_{Sym} and L_{Sym} and free boundary conditions elsewhere. Conditionally this probability is an upper bound for another probability supported over Sym, as

$$\mu[\gamma_1 \overset{\Omega}{\longleftrightarrow} \gamma_2 \mid \Gamma_{2_j} = \gamma_1 \ \& \ \Gamma_{2_{j+2\delta'}} = \gamma_2, k_{\gamma_1} = k_{\gamma_2}] \geq \mu_{\Omega}^{\{\gamma_1,\gamma_2\}}[\ \gamma_1 \longleftrightarrow \gamma_2\ ] \ , \tag{$\bigstar$}$$

with the conditioning on the connected components applying to $+/-$ spin configurations as shown in *Figure 3*, Ω is a region inside the symmetric domain (see *Figure 5*), and the $\{\gamma_1, \gamma_2\}$ superscript indicates boundary conditions wired along γ_1 and γ_2. Similarly, conditional on $\Gamma_{2_j} = \gamma_1$ & $\Gamma_{2_{j+2\delta'}} = \gamma_2$, $\{\gamma_1 \overset{\Omega}{\longleftrightarrow} \gamma_2\}$ occurs. To quantify the probability of $\mathscr{C}_{2_{j+\delta'}} \setminus (C_0 \cup C_2)$, conditionally that the connect components of the event not intersect those of $\mathscr{C}_{2_j} \cap \mathscr{C}_{2_{j+2\delta'}}$, we introduce modifications through ($\mathcal{S}$ SMP), which impact the boundary conditions of the symmetric domains that will be constructed, while modifications through ($\mathcal{S}$ CBC) impact the number of paths that can be averaged over in Γ_{2_j} and $\Gamma_{2_{j+2\delta'}}$ given the occurrence of C_0.

In particular, under the weaker form of the Spatial Markov Property, we can push boundary conditions away from nonempty boundary ∂ Sym $\subset \partial H_j$ with the edge of intersection towards L_{Sym}, to then construct Sym by reflecting one half of the region enclosed by the realizations $\{\gamma_1, \gamma_2\} \subset \mathscr{C}_{2_j} \cap \mathscr{C}_{2_{j+2\delta'}}$, as follows. Because the event $\mathscr{C}_{j+\delta'}$ necessarily induces the existence of a loop configuration from $\mathcal{S}_j$ to 2_j, under Dobrushin boundary conditions which stipulate the existence of a wired arc of length $\frac{\pi}{6}$ along 2_j, the distribution μ on loop configurations satisfying $\mathscr{C}_{2_j}$ implies that the probability of a crossing across Sym supported on $\mu^{\text{mix}}_{\text{Sym}}$ [2]. With wired boundary conditions along two sides of Sym, comparison between boundary conditions, and monotonicity, of the loop measure imply, under the circumstance of , that the pushforward of the conditionally defined crossing events under μ with dominate other boundary conditions on Sym.

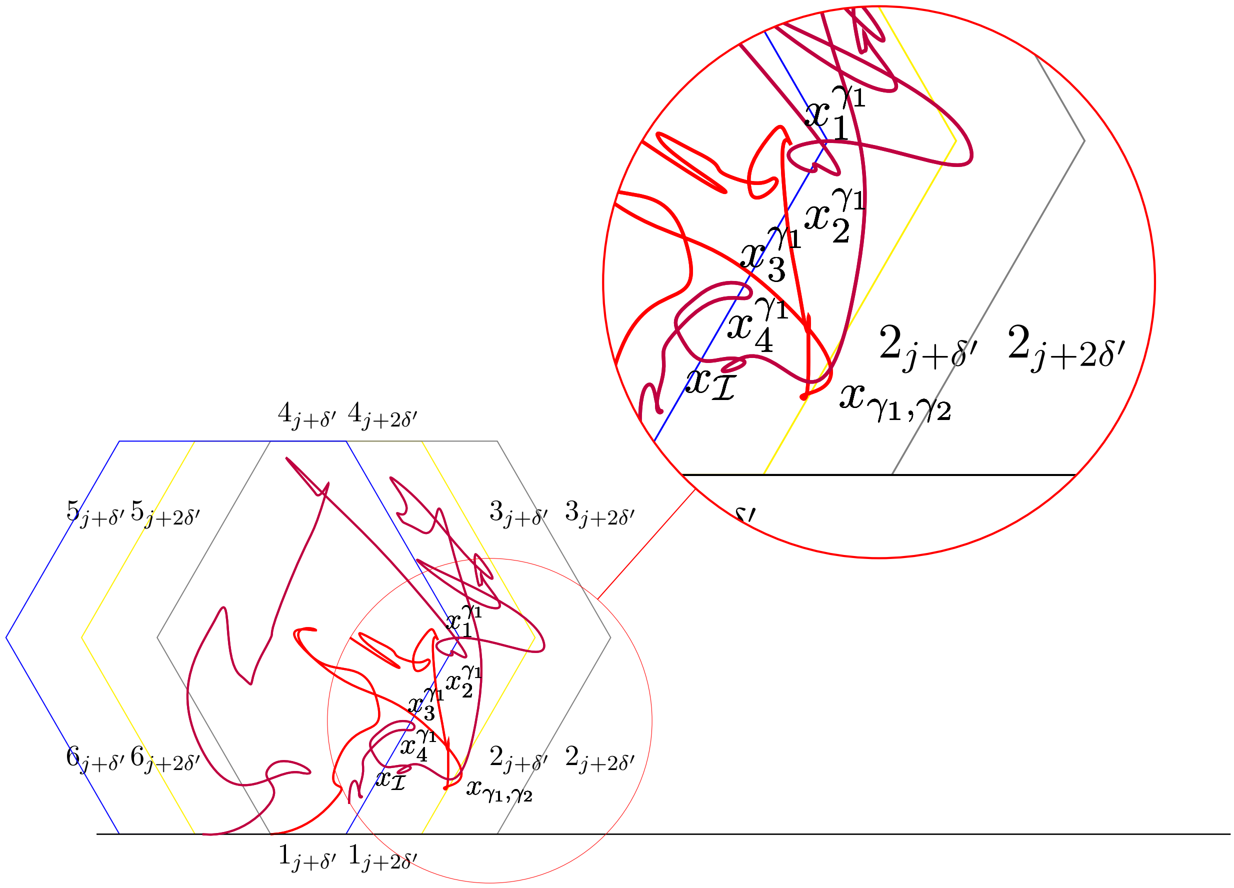

Figure 3: Sym *construction from macroscopic* $+\backslash-$ *crossings induced by* $\mathscr{C}_{2_j}$ *and* $\mathscr{C}_{2_{j+2\delta'}}$. *Loop configurations with distribution* $\boldsymbol{P}$, *with corresponding* $+/-$ *random coloring of faces in* $\boldsymbol{H}$ *with distribution* μ, *are shown with purple* γ_1 *and red* γ_2. *Each configuration intersects* 2_j, *with crossing events occurring across the box* H_j *and its translate* $H_{j+2\delta'}$. *Under translation invariance of the spin representation, different classes of* Sym *domains are produced from the intersection of* γ_1 *and* γ_2, *as well as the connected component of an intersection* $x_{\mathcal{I}}$ *incident to* 2_j, *which is shown above the second intersection of the red connected components of* γ_2. *From one such arrangement of* γ_1 *and* γ_2, *a magnification of the symmetric domain is provided, illustrating the contours of* Sym *which are dependent on the connected components of the outermost* γ_2 *path above* x_{γ_1,γ_2}, *while the connected components of* γ_2 *below* x_{γ_1,γ_2} *determine the number of connected components below the intersection. Across* 2_j, *one half of* Sym *is rotated to obtain the other half about the crossed edge. From paths of the connected components of each configuration,* Sym *is determined by forming the region from the intersection of the connected components of* γ_1 *and* γ_2 *in the magnified region. We condition on the number of connected components of each path by stipulating that they are equal to form two connected sets along the incident boundary to* Sym. *At the point of intersection between the red and purple* $+/-$ *spin configurations, the connected component associated with* $x_{\mathcal{I}}$ *determines half of the lowest side of* Sym. *The region allows for the construction of identical domains under* $\mathscr{C}_{5_j}$ *and* $\mathscr{C}_{5_{j+2\delta'}}$. *Connected components are only shown in the vicinity of* 2_j *for the identification of boundaries of* Sym, *running from the intersection of* γ_2 *at the cusp of* 2_j *and* 3_j, *and from two nearby intersections of* γ_1 *with* 2_j. *The points of intersection of the purple connected components of* γ_1 *with* 2_j *are labeled* $x_1^{\gamma_1}, x_2^{\gamma_1}, x_3^{\gamma_1}, x_4^{\gamma_1}, x_{\mathcal{I}}$.

[2]The mix boundary conditions are provided in two separate constructions of Sym below.

Notably, boundary conditions are pushed forwards in the following partitions of hexagons incident with the boundary. We introduce equal partitions of the boundary through a $+/-$ coloring of the outermost layer of hexagons in finite volume domains. To partition vertices in Sym to then apply ($\mathcal{S}$ SMP), we assign $+$ boundary conditions to a partition of the first layer of hexagons outside of a loop configuration induced by $\mathscr{C}_{2_{j+\delta'}} \backslash (C_0 \cup C_2)$, conditioned under realizations γ_1 & γ_2 sampled under μ, as follows. Given such a crossing, the length of the boundary of Sym is entirely determined by the number of connected components of the spin configuration, which corresponds to the the edges of the spin configuration between neighboring hexagons that are colored $+$ and $-$. Next, we partition the outermost layer of hexagons outside of the paths above and below the intersection of the connected components of γ_1 and γ_2 (see *Figure 3* for loop configurations in red and purple sampled under μ whose connected components after intersection with 2_j yield boundaries of Sym). Without loss of generality, if we assume that the connected component of γ_1 in a neighborhood of 2_j is closer to the edge $2_{j+\delta'}$ than those of γ_2, we take the connected components of γ_1 closest to $2_{j+\delta'}$ to construct one half of the top of Sym. The other top half of Sym will be readily obtained by reflection through 2_j, as will the remaining one half of the lower part. Below x_{γ_1,γ_2}, without loss of generality the connected components of γ_2 constitute one half of the lower region of Sym. Before reflection one half of Sym is constructed by taking the union $\gamma_1^{x_{\gamma_1,\gamma_2}} \cup \gamma_2^{x_{\gamma_1,\gamma_2}}$, where the paths in the union denote the restriction of the connected components of γ_1 and γ_2 after $\mathscr{C}_j$ and $\mathscr{C}_{j+2\delta'}$ have occurred, given one specification stated below on the number of connected components of $\gamma_1^{x_{\gamma_1,\gamma_2}}$ relative to those of $\gamma_2^{x_{\gamma_1,\gamma_2}}$. The accompanying reflections $\tilde{\gamma}_1^{x_{\gamma_1,\gamma_2}}$ and $\tilde{\gamma}_2^{x_{\gamma_1,\gamma_2}}$ give the other half of Sym. Finally, we denote $x_{\mathcal{I}}$ as another point of intersection of γ_1 (γ_2) with 2_j besides the intersection of $\gamma_1^{x_{\gamma_1,\gamma_2}}$ ($\gamma_2^{x_{\gamma_1,\gamma_2}}$) determining the height of Sym (see *Figure 3* for multiple intersection points of the red and purple spin configurations with 2_j).

5.1.1 First partition of the incident hexagonal layer to the Sym boundary

Besides the construction of Sym from the connected components, it remains to detail how the spins are distributed along the boundary. Under the relaxation ($\mathcal{S}$ SMP), symmetric domains can only be constructed when the number of connected components of γ_1 above x_{γ_1,γ_2} equals those of γ_2 below x_{γ_1,γ_2}. Under this hypothesis, the first partition of the first layer of hexagons outside of the connected components of Sym can be achieved by assigning $+$ spins to the first layer bordering the restriction of connected components of $\gamma_1^{x_{\gamma_1,\gamma_2}}$, while $-$ spins can be assigned to the bordering first layer of the restriction of connected components of $\gamma_2^{x_{\gamma_1,\gamma_2}}$. Under this assignment, one half of Sym can be readily constructed by reflection across 2_j. The intersection of the connected components at x_{γ_1,γ_2} establishes the proportion of $+$, or $-$, signs that are distributed in between 2_j and $2_{j+\delta'}$. With the first partition of the layer incident to the boundary of Sym, we accommodate ($\mathcal{S}$ SMP) by assigning $+$ boundary conditions, with a $-$ assignment of boundary conditions to the remaining connected components of γ_2 below x_{γ_1,γ_2}. Finally, we reflect the region across 2_j to obtain the resulting domain which has wired boundary conditions along its top arc, and free boundary conditions along its bottom arc. ($\mathcal{S}$ CBC) will be invoked through a comparison of a slighly altered Sym with wired boundary conditions along the entirety of the union of connected components of $\gamma_1^{x_{\gamma_1,\gamma_2}} \cup \gamma_2^{x_{\gamma_1,\gamma_2}}$ and hence along the whole domain itself.

5.1.2 Second partition of the incident hexagonal layer to the Sym boundary

We present a second partition of the incident layer to the boundary of Sym under the spin flip $\sigma \mapsto -\sigma$. In contrast to the first vertex partition above, the second partition achieves a partition of the incident layer to the connected components with the assignment of $-$ spins along $\gamma_1^{x_{\gamma_1,\gamma_2}}$, and $+$ spins assigned along $\gamma_2^{x_{\gamma_1,\gamma_2}}$, inducing free boundary conditions along the top half of Sym and wired boundary conditions along the bottom half of Sym (see *Figure 4*). The remaining half of symmetric domains corresponding to the second partition of $\gamma_1^{x_{\gamma_1,\gamma_2}} \cup \gamma_2^{x_{\gamma_1,\gamma_2}}$ can similarly be constructed through reflection.

5.2 Incorporating ($\mathcal{S}$ CBC)

We progress towards making use of another modification for the dilute Potts model through the two types of symmetric domains above to ensure that such domains are conditionally bridged with good probability. We make use of the comparison through the following modification of Sym.

5.2.1 Modification to boundary conditions induced by the first partition of the Sym incident layer

A first modification of the incident hexagonal layer can be realized by taking the first partition presented, through a modification of the $+$ spin assignment along the incident layer bordering $\gamma_1^{x_{\gamma_1,\gamma_2}}$ uniformly to $-$ spins, while leaving the $-$ spin assignment to the incident layer bordering $\gamma_2^{x_{\gamma_1,\gamma_2}}$ fixed. This construction yields a class of symmetric domains with free boundary conditions along the entire boundary before reflecting to obtain the other half.

5.2.2 Modification to boundary conditions induced by the second partition of the Sym incident layer

A second modification of the incident hexagonal layer can be realized by taking the second partition presented, through a modification of the $-$ spin assignment along the incident layer bordering $\gamma_2^{x_{\gamma_1,\gamma_2}}$ uniformly to $+$ spins, while leaving the $+$ spin assignment to the incident layer bordering $\gamma_1^{x_{\gamma_1,\gamma_2}}$ fixed. This construction yields a class of symmetric domains with wired boundary conditions along the entire boundary before reflecting to obtain the other half which inherits wired boundary conditions.

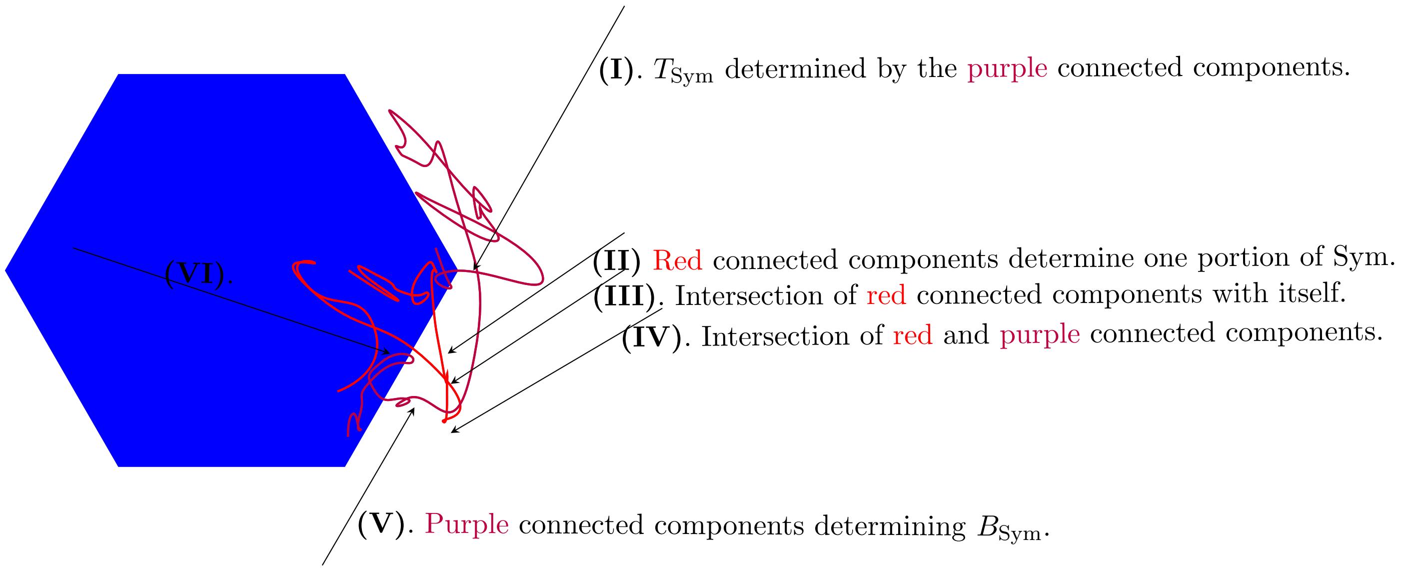

Figure 4: Sym *from Figure 3, incident to* 2_j*. The region in between the connected components of each path constitute the boundaries of the symmetric region. Arrows are shown to each connected component which are used to construct* Sym *given relevant connected components of* γ_1 *and* γ_2*. The non trivial intersection of the red and purple connected components within the blue interior of* H_j *determine one half of* Sym *before reflection.* **(I)** *illustrates the top side of* Sym *determined by the intersection of the purple connected components with itself.* **(II)** *illustrates a portion of* Sym *that is reflected about* 2_j *to obtain the other half of* Sym*.* **(III)** *illustrates the intersection of red connected components with itself.* **(IV)** *illustrates the intersection of connected components from* γ_1 *and* γ_2 *which are removed from the interior of* Sym*.* **(V)** *illustrates the purple connected components determining* $\mathrm{B}_{\mathrm{Sym}}$*.* **(VI)** *illustrates the red connected components that are removed from the interior of* Sym*, upon multiple intersection points with* 2_j*.*

Next, we make use of the two types of Sym domains, in addition to the modification of boundary conditions as follows. From an application of ($\mathcal{S}$ CBC), the conditional probability introduced at the beginning of the proof, under spin configurations supported on μ_{Sym} satisfies,

$$\mu[\mathscr{C}_{2_j}\backslash(C_0 \cup C_2) \mid \Gamma_{2_j} = \gamma_1 \ \&\ \Gamma_{2_{j+2\delta'}} = \gamma_2, k_{\gamma_1} = k_{\gamma_2}] \leq \mu_{\Omega}^{\{\gamma_1,\gamma_2\}^c}[\mathscr{C}_{j+\delta'} \mid \gamma_1 \cap \gamma_2 = \emptyset, \gamma_1 \cap \gamma_3 = \emptyset, k_{\gamma_1} = k_{\gamma_2}\ ] \ ,$$

after examining the pushforward of the conditional probability above under spin configurations supported in Sym, where the superscript $\{\gamma_1,\gamma_2\}^c$ denotes free boundary conditions along γ_1 and γ_2 and wired elsewhere, the complement of $\{\gamma_1,\gamma_2\}$ given in the lower bound of $\bigstar$. The stochastic domination above of the conditional probability under no boundary conditions on any side of Sym will be studied for paths $\gamma_3 \in \Gamma_{j+\delta'}$. The event under $\mu_{\Omega}^{\{\gamma_1,\gamma_2\}^c}$ demands that the connected components of γ_3 be disjoint for those of γ_1 and γ_2 for the entirety of the path.

Particularly, we remove the conditioning from the pushforward in the upper bound because the definition of Ω implies that connectivity holds in between γ_1 and γ_2. Pointwise, the connected components of γ_3 do not intersect those of γ_1 and γ_2. Recalling $\bigstar$ in *5.1*, we present additional modifications to the renormalization argument through the lower bound of the inequality to exhaust the case for $\mathcal{C}_j \equiv \mathscr{C}_{2_j}$. Lower bounds for the pushforward under μ_Ω can only be obtained for mixed boundary conditions along Sym precisely under partitions of the incident hexagonal layer given in *5.1.1* & *5.1.2*.

Under the conditions of ($\mathcal{S}$ SMP), crossings in Ω with boundary conditions $\{\gamma_1,\gamma_2\}$, the lowermost bound for $\bigstar$ can only be established when boundary conditions are distributed under *5.1.1* or *5.1.2*. For completeness, we first establish the lower bound for *5.1.1*, in which the boundary conditions for a crossing distributed under $\mu_{\mathrm{Sym}}^{\{\gamma_1,\gamma_2\}}$ can be compared to a closely related crossing distributed under $\mu_{\Omega}^{\{\gamma_1,\gamma_2\}^c}$.

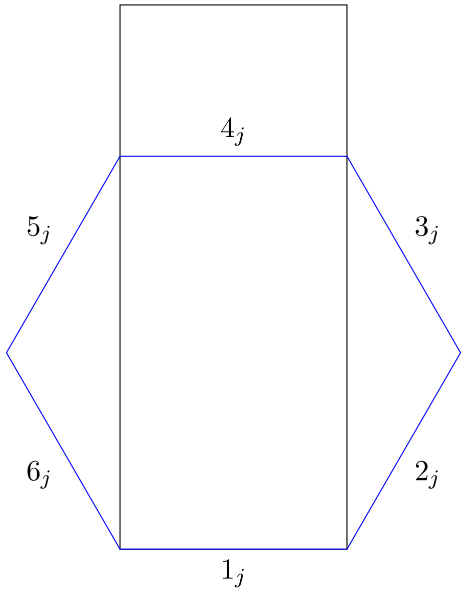

Figure 5: *Crossing events through paths to the topmost edge 4_j, in addition to Ω and its subsets from the partition are indicated. By construction, the three partitions of 1_j from which the top to bottom crossings occur begin respectively from $\mathcal{S}_j$, $\mathcal{S}_{j+\delta'}$ and $\mathcal{S}_{j+2\delta'}$. Connectivity induced by $\mathscr{C}_{4_{j+\delta'}}$ occurs in $\Omega_{(L\cup R)^c}$.*

To establish the comparison, the edges in $\mathrm{Sym} \cap \Omega$, we divide the proof into separate cases depending on whether the boundary conditions for vertcies along γ_1 or γ_2 are connected together under wired or free boundary conditions. For $\mathcal{C}_j \equiv \mathscr{C}_{2_j}$, one instance of pushing boundary conditions occurs when , while another instance of pushing boundary conditions occurs when $\mathcal{C}_j \equiv \mathscr{C}_{4_j}$ in Section *5.4*. [3]

5.2.3 Pushing boundary conditions away towards Sym from Ω in the first partition of the incident layer

One situation occurs as follows. It is possible that $+\backslash-$ configurations distributed under μ_Ω can be compared to configurations distributed under μ_{Sym} by pushing boundary conditions away from the first partition of Sym towards Ω; applying ($\mathcal{S}$ CBC) between deterministic and random circuits, under the conditional measure $\mu \equiv \mu[\ \cdot |_E \ |\ \ ]$, yields

$$\mu[\ ] \leq \mu[\ ]\ ,$$

by virtue of monotonicity in the domain, ($\mathcal{S}$ SMP), and duality. Additionally,

$$,$$

by virtue of

5.2.4 Pushing boundary conditions away towards Sym from Ω in the second partition of the incident layer

Under $\frac{2\pi}{3}$ rotational invariance of μ, the argument for this case can be directly applied with $\mathcal{C}_j \equiv \mathscr{C}_{5j}$. Examining the pushforward of this crossing event, in addition to $\mathscr{C}_{5_{j-\delta'}}$ which guarantees the existence of a connected component that necessarily crosses 5_j through $5_{j-\delta'}$, leads to the same conclusion with wired boundary conditions from to along Sym. Under duality, the identification between measures under Dobrushin boundary conditions over Sym applies. Hence a combination of ($\mathcal{S}$ SMP), followed by ($\mathcal{S}$ CBC), implies that $\{L_{\mathrm{Sym}} \longleftrightarrow R_{\mathrm{Sym}}\}$ occurs with substantial probability.

[3] In contrast to the planar case of [14], considerations through the condition $k_{\gamma_1} = k_{\gamma_2}$ impact the construction of Sym and the rotational symmetry that it enjoys.

5.3 $\mathcal{C}_j \equiv \mathscr{C}_{3_j}$

In the second case, one can apply similar arguments with the following modifications. To identify other possible symmetric regions Sym corresponding to $\mathscr{C}_{3_j}$ and $\mathscr{C}_{3_{j+2\delta'}}$, fix path realizations $\gamma_1 \in \Gamma_{3_j}$ and $\gamma_2 \in \Gamma_{3_{j+2\delta'}}$ (see *Figure 2* for yellow connected components in the Sym construction). From γ_1 and γ_2, we construct Sym by reflecting half of the domain across 3_j instead of 2_j. Under $\frac{2\pi}{3}$ rotational invariance of μ, Sym constructed in this case correspond to symmetric domains induced by the paths in $\mathscr{C}_{5_j}$ and $\mathscr{C}_{5_{j+2\delta'}}$. Applying the same argument to push bondary conditions away from wired boundary conditions on 3_j (5_j), to L_{Sym} (R_{Sym}) establishes the same sequence of inequalities, through contributions of μ, μ & μ_{Sym}. Sym for $\mathscr{C}_{3_j}$ corresponds to rotating the crossings of loop configurations, and hence the symmetric region to 5_j from the symmetric domain corresponding to 2_j in *Figure 3*.

5.4 $\mathcal{C}_j \equiv \mathscr{C}_{4_j}$

In the third case, we denote the events C_0 and C_2 as bottom to top crossings, respectively across H_j and $H_{j+2\delta'}$, with respective path realizations Γ_1 and Γ_1 as in the previous two cases. However, the final case for top to bottom crossings stipulates that the construction of Sym not depend on Ω. We introduce a square symmetric region as in [14] but present modifications to how the points to the left and right of γ_1 and γ_2 are partitioned. In particular, we denote Ω as the collection of all points in the rectangular Sym, along with the partition $\Omega = \Omega_L \cup \Omega_{(L\cup R)^c} \cup \Omega_R$. In the partition, each set respectively denotes the points to the left of γ_1, the points in between the left of γ_1 and the right of γ_2, and the points to the right of γ_2. With some abuse of notation we restrict the paths in Ω_L, Ω_R and $\Omega_{(L\cup R)^c}$ to coincide with crossings inside Sym itself, in which $\Omega_R \equiv \mathrm{Sym} \cap \Omega_R$, $\Omega_L \equiv \mathrm{Sym} \cap \Omega_L$, and $\Omega_{(L\cup R)^c} \equiv \mathrm{Sym} \cap \Omega_{(L\cup R)^c}$. We provide such an enumeration to apply ($\mathcal{S}$ SMP) and then ($\mathcal{S}$ CBC), when comparing the spin representation measures supported over Ω and Sym.

Besides the Ω partition, to apply ($\mathcal{S}$ SMP) we examine $\mathcal{R}_1 \equiv (\mathrm{Sym} \backslash H_j^c) \cap \Omega_L$ and $\mathcal{R}_2 \equiv (\mathrm{Sym} \backslash H_j^c) \cap \Omega_R$ which denote the collection of points to the left of γ_1 and to the right of γ_2 in the region above H_j that is contained in Sym (see *Figure 5*). For ($\mathcal{S}$ CBC), it is necessary that we isolate $\mathcal{R}_1$ and $\mathcal{R}_2$ so that ($\mathcal{S}$ CBC) can be applied to the outermost layer of hexagons incident to $\partial\, \Omega$ through similar partitions of the incident layer.

Along this layer,

5.4.1 Pulling boundary conditions back from towards

Under $\frac{2\pi}{3}$ rotational invariance of the spin measure μ, no reflection translates of $\mathscr{C}_{4_j}$ events produce additional symmetric domains.

In *Figure 5*, the Ω partition is illustrated. For $\mathscr{C}_{4_j}$ type events, we denote

□

6 Wired boundary conditions induced by vertical crossings

To analyze

7 References

[1] Beffara, V. & Duminil-Copin, H. The self-dual point of the two-dimensional random-cluster model is critical for $q \geq 1$. *Probability Theory and Related Fields* **153** 511-542 (2012).

[2] Beliaev, D., Muirhead, S. & Wigman, I. Russo-Seymour-Welsh estimates for the Kostlan ensemble of random polynomials. *Arxiv* (2017).

[3] Crawford, N., Glazman, A., Harel, M. & Peled, R. Macroscopic loops in the loop $O(n)$ model via the XOR trick. *Arxiv* (2020).

[4] Clarence, J., Damasco, G., Frettloh, D.,. Loquias, M. Highly Symmetric Fundamental Domains for Lattices in $\mathbf{R}^2$ and $\mathbf{R}^3$. *Arxiv* (2018).

[5] Duminil-Copin, H. Parafermionic observables and their applications to planar statistical physics models. *Ensaois Matematicos* **25** 1-371 (2013).

[6] Duminil-Copin, H. Parafermoionic observables and their applications. *AMP Bulletin* (2015).

[7] Duminil-Copin, H. Sharp threshold phenomena in statistical physics. *Japanese Journal of Mathematics* **14** 1-25 (2019).

[8] Duminil-Copin, H., Glazman, A., Peled, R. & Spinka, Y. Macroscopic Loops in the Loop $O(n)$ model at Nienhuis' Critical Point. *Arxiv.*

[9] Duminil-Copin, H., Hongler, C. & Nolin, P. Connection probabilities and RSW-type bounds for the FK Ising Model. *Communications on Pure and Applied Mathematics* **64**(9) (2011).

[10] Duminil-Copin, H., Manolescu, I. & Tassion, V. Planar random-cluster model: fractal properties of the critical phase. *Arxiv* (2020).

[11] Duminil-Copin, H. & Smirnov, S. Conformal invariance of lattice models. *Arxiv* (2012).

[12] Duminil-Copin, H. & Smirnov, S. The convective constant of the honeycomb lattice equals $\sqrt{2+\sqrt{2}}$. *Annals of Mathematics* **175**(3) 1653-1665 (2012).

[13] Duminil-Copin, H., Sidoravicius, V. & Tassion, V. Continuity of the phase transition for planar random-cluster and Potts models for $1 \leq q \leq 4$. *Communications in Mathematical Physics* **349** 47-107 (2017).

[14] Duminil-Copin, H. & Tassion, V. Renormalization of crossing probabilities in the planar random-cluster model. *Arxiv.*

[15] Feher, G. & Nienhuis, B. Currents in the dilute $O(n = 1)$ model. *Arxiv* 1510.02721v2 (2018).

[16] Fradkin, E. Disorder Operators and their Descendants. *Lecture Notes.*

[17] Glazman, A. & Manolescu, I. Uniform Lipschitz functions on the triangular lattice have logarithmic variations. *Arxiv* (2019).

[18] Gheissari, R. & Lubetzky, E. Quasi-polynomial Mixing of Critical two-dimensional Random Cluster Models. *Random Structures & Algorithms* **56**(2) (2019).

[19] Guo, W., Blote, H. & Nienhuis, B. First and Second Order Transitions in the Dilute $O(n)$ models *International Journal of Modern Physics* **10**(1) 291-300 (1999).

[20] Guo, W., Blote, H. & Nienhuis, B. Phase Diagram of a Loop on the Square Lattice. *International Journal of Modern Physics* **10**(1) 301-308 (1999).

[21] Hongler, C. Percolation on the triangular lattice. *Arxiv* (2007).

[22] Nienhuis, B. & Guo, W. Tricritical $O(n)$ models in two dimensions. *American Physical Society* **78**, 061104 (2008).

[23] Russo, L. A note on percolation. *Zeitschrift fur Wahrscheinlichkeitstheorie und Verwandte Gebiete* **43** 39-48 (1978).

[24] Seymour, P. & Welsh, D. Percolation probabilities on the square lattice. *Annals Discrete Math*, **3** 227–245 (1978).

[25] Smirnov, S. Discrete Complex Analysis and Probability. *Proceedings of the International Congress of Mathematicians* (2010).

[26] Smirnov, S. Conformal invariance in random cluster models. I. Holomorphic fermions in the Ising model. *Annals of Mathematics* **172** 1435-1467 (2010).

[27] Tassion, V. Crossing probabilities for Voronoi percolation. *The Annals of Probabilitiy* **44**(5) 3385-3398 (2016).

[28] Zeng, X. A Russo Seymour Welsh Theorem for critical site percolation on $\mathbf{Z}^2$. *Arxiv* (2013).